High-Throughput Permeability pH Profile and High-Throughput Alkane/Water log *P* with Artificial Membranes

Frank Wohnsland and Bernard Faller*

Novartis Pharma AG, WKL-122.P.33, CH-4002 Basel, Switzerland

Received July 3, 2000

This study reports on a novel, high-throughput assay, designed to predict passive, transcellular permeability in early drug discovery. The assay is carried out in 96-well microtiterplates and measures the ability of compounds to diffuse from a donor to an acceptor compartment which are separated by a 9−10 μm hexadecane liquid layer. A set of 32 well-characterized, chemically diverse drugs was used to validate the method. The permeability values derived from the flux factors between donor and acceptor compartments show a good correlation with gastrointestinal absorption in humans. For comparison, correlations based on experimental or calculated octanol/water distribution coefficients (log $D_{o/w,6.8}$) were significantly lower. In addition, this simple and robust assay allows determination of pH permeability profiles, critical information to predict gastrointestinal absorption of ionizable drugs and difficult to obtain from cell culture experiments. Correction for the unstirred water layer effect allows to differentiate between effective and intrinsic membrane permeability and opens up the dynamic range of the method. In addition, alkane/water partition coefficients can be derived from intrinsic membrane permeabilities, making this assay the first high-throughput method able to measure alkane/water log *P* in the microtiterplate format.

Introduction

The absorption of orally administered substances is largely determined by their ability to cross the gastrointestinal tract (GI-tract). Around one-third of development candidates is lost due to inappropriate pharmacokinetic properties.[1] To increase the quality of "research" compounds, methods are required in early drug discovery to dissect key factors influencing drug absorption like solubility and permeability, the two components of the Biopharmaceutics Classification Scheme[2] (BCS).[3] A number of molecular properties influencing passive absorption of drugs have been identified. These include octanol/water partition and distribution coefficients (log *P*/*D*), ionization state (pK_a), hydrogen bond potential, and molecular size. Although these parameters have proven to be useful to predict passive absorption, their impact in early drug discovery has been limited due to the amount of material, manpower, and time needed to generate these data. In addition, semiempirical relations linking octanol/water log *P*/*D* to absorption, although successful in many subsets, often break down when noncongeneric structures are analyzed − mainly due to the inappropriate hydrogen bond acidity component of octanol.[4−6]

Alternatively, cell culture models such as Caco-2 cell monolayers[7,8] have proven useful to predict gastrointestinal drug absorption. This method is, however, rather labor-intensive, limited to a narrow pH range, and not easily applicable for high-throughput. In addition, the dynamic range of cell-based assays is restricted due to thick unstirred water layers (unstirred cell cultures). Another promising approach to permeability screen lies in permeation assays where a chemical or biochemical barrier is used to mimic the physicochemical properties of phospholipid bilayers. In 1997, Camenisch et al. reported on correlation between fraction absorbed and flux measured with artificial membranes made of cellulose filters impregnated with bulk octanol.[9] More recently, following numerous studies which demonstrated the possibility to form artificial phospholipid bilayer membranes[10−13] and the possibility to stabilize them using microporous filters,[14,15] Kansy et al. proposed a model membrane permeation assay consisting of filters coated with an alkane solution of lecithin.[16] One drawback of this assay, however, lies in the structure and thickness (120 μm) of the supporting filter which renders the formation of well-characterized bilayer membranes rather unlikely. In addition, these membranes might be prone to assay variations depending on the quality of the phospholipids and how successful the lipid layers form.

It has been demonstrated that for neutral substances the main contributors to membrane permeability are molecular size and hydrogen-bonding capability of the solute.[17] If one considers the molecular weight range 200−600 which covers the large majority of drug candidates, membrane permeability becomes essentially a matter of hydrogen bond potential. Experimental determination of hydrogen bond potential is usually obtained by comparing partition coefficients in octanol and alkane (Δlog *P*).[5] In practice, however, log *P* alkane values are often difficult to measure because of the low solubility of most compounds in alkane/water.

In this paper, we report on a new permeation assay based on a 9−10 μm hexadecane liquid layer immobilized between two aqueous compartments. This method is the first high-throughput assay able to

* To whom correspondence should be addressed. Tel: +41 61 696 5406. Fax: +41 61 696 8663. E-mail: bernard.faller@pharma.novartis.com.

10.1021/jm001020e CCC: $20.00
Published on Web 02/03/2001

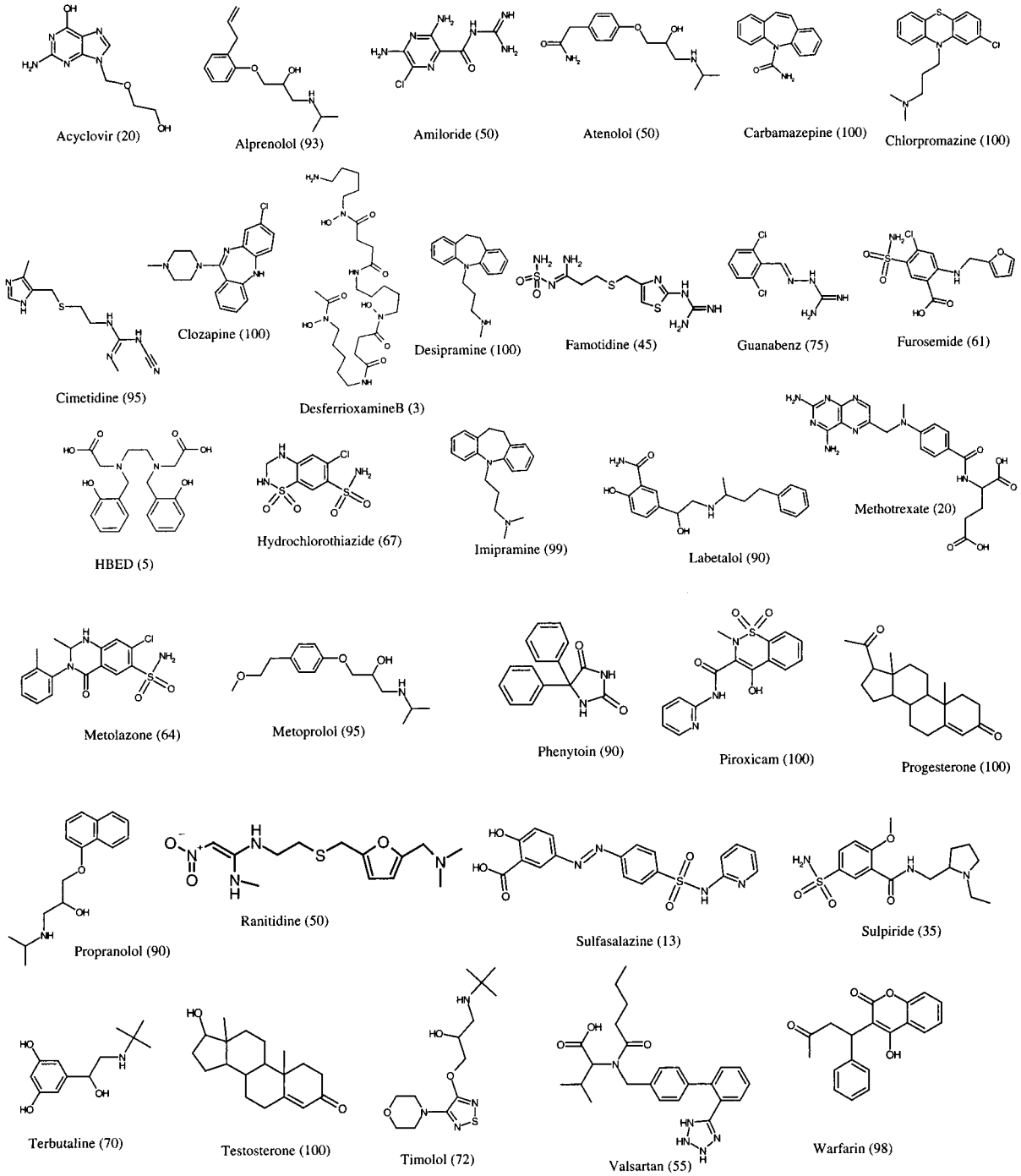

Figure 1. Chemical structures of generic drugs used to correlate log P_e with GI-tract absorption. Percent absorption values in humans are indicated in parentheses.

generate large numbers of experimental data on permeability pH profiles and alkane/water partition coefficients.

Experimental Section

Chemicals. All generic drugs (Figure 1) were purchased from Sigma (Division of Fluka Chemie AG, Buchs, Switzerland) except valsartan (Diovan), desferrioxamine B (Desferal), and HBED which were synthesized in-house. Compounds were dissolved in dimethyl sulfoxide (DMSO) at a concentration of 10 mg/mL each and used without further purification. DMSO was purchased from Merck AG (Dietikon, Switzerland) with a purity grade >99.8%. Hexane and hexadecane were purchased from Fluka with purity grades >99% and >98%, respectively. The buffers for pH values in the pH range 6−8 were made from a pH 7.0 phosphate buffer (28 mM KH_2PO_4 and 41 mM Na_2HPO_4), adjusted to the respective pH values with NaOH (pH 8.0) or H_3PO_4 (pH 6 and 6.8). For acidic pH values (3−5.5), 50 mM acetate buffer was used. Alkaline pH values (8.5−10) were obtained from a pH 9.0 Borax buffer (43 mM disodium tetraborate, 17 mM KH_2PO_4), adjusted with H_3PO_4 or NaOH.

Methods. Permeation experiments were carried out in 96-well microtiter filter plates obtained from Millipore AG (Volketswil, Switzerland). Filter (isopore, polycarbonate) specifications were as follows: 3 μm pore size, 9−10 μm thickness, and 5−20% porosity. Each well of the filter plate was impregnated with 15 μL of 5% hexadecane dissolved in hexane (i.e., total amount of hexadecane: 0.75 μL) for at least 10 min to allow for complete evaporation of the hexane. Subsequently, the donor compartments were hydrated with 300 μL of 50 μg/

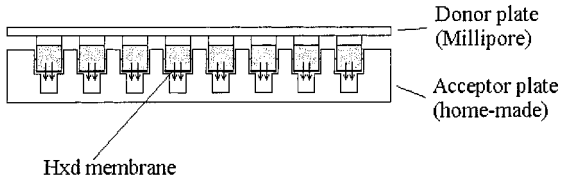

Figure 2. Schematic principle of the hexadecane permeability assay.

mL test compound in buffer, containing 5% DMSO and 100 mM KCl, and connected to a homemade Teflon acceptor plate which had been prefilled with buffer containing 5% DMSO. The resulting sandwich construct (Figure 2) was incubated at room temperature under constant light shaking (50−100 rpm). After 5 h, the sandwich was disassembled and the solution in the acceptor was transferred to a disposable UV-transparent plate (Corning Costar, Corning, NY). UV absorption was measured with a SPECTRAmax190 microplate spectrophotometer (Molecular Devices Corp., Sunnyvale, CA) at absorption wavelengths between 260 and 290 nm.

To ensure that the donor/acceptor fluxes were not due to porous or unstable hexadecane layers, the stability of the hexadecane membranes was tested at the end of the incubation period by electrical resistance measurements. Wells with barriers which displayed electrical resistance lower than 5 kΩ were discarded. Electrical resistance measurements were performed using a Keithley 6517A electrometer (Keithley Instruments S.A., Dübendorf, Switzerland) with Ag/AgCl electrodes from World Precision Instruments (Berlin, Germany).

Ionization constants were measured by potentiometric titration in 0.15 M KCl at 25.0 °C using a GlpKa instrument (Sirius Analytical Instruments, Forest Row, U.K.). Partition and distribution coefficients were measured using the pH metric technique using a PCA101 automatic titrator (Sirius Analytical Instruments, Forest Row, U.K.). This technique basically consists of two linked titrations: a normal titration followed by a two-phase titration in the presence of the partition solvent.[18,19]

Polar surface area (PSA) is a surface descriptor which has been introduced some years ago as an alternative to calculated octanol/water partition coefficients to measure permeability of drugs.[20−23] PSA is defined as part of the surface area contributed by nitrogen, oxygen, and connected hydrogen atoms. In this study we calculated PSA using the approach published by Palm et al.[21]

In silico octanol/water distribution coefficients at pH 6.8 (clog $D_{6.8}$) were calculated from pK_a and log P with pKaLOGP version 5.1 (Sirius Analytical Instruments, Forest Row, U.K.). Ionization constants were calculated with ACD pKa DB and partition coefficients with MedChem CLOGP.

Data Evaluation. At the end of the incubation period the sandwich was carefully disassembled, the acceptor plate measured with the UV microtiter plate spectrophotometer, and the donor plate submitted to current measurements to assess the integrity of the hexadecane membranes.

The apparent permeability value P_a is determined from the ratio r of the absorbance of compound found in the acceptor chamber divided by the theoretical equilibrium absorbance (determined independently):

$$P_a = -\frac{V_D \quad V_R}{(V_D + V_R)At} \cdot \ln(1 - r) \qquad (1)$$

In this equation, V_R is the volume of the acceptor compartment (0.4 cm^3), V_D is the donor volume (0.3 cm^3), A is the accessible filter area (total filter area, 0.24 cm^2, multiplied by a porosity ratio of 20%), and t is the incubation time. Equation 1 is obtained from the differential equation[24]

$$\frac{dc_R}{dt} = \frac{P_a A}{V_R}(c_D - c_R) \qquad (2)$$

Table 1. Fraction Absorbed in the GI-Tract, HDM Permeability Data at pH 6.8, Highest HDM Permeability Observed between pH 4−8, and Octanol/Water Distribution Coefficients for the 32 Generic Substances as Shown in Figure 3

compound	% fraction absorbed	log P_e (cm/s) at pH 6.8	log P_e (cm/s) at pH 4−8	exptl log $D_{6.8}$
acyclovir	20	−4.8	−4.8	−2
alprenolol	93	−4.0	−4.0	0.3
amiloride	50	−4.6	−4.4	−2.1
atenolol	50	−4.5	−4.5	−2.5
carbamazepine	100	−3.9	−3.9	2.4
chlorpromazine	100	−3.7	−3.5	2.9
cimetidine	95	−4.0	−4.0	0.1
clozapine	100	−3.6	−3.6	3
desferrioxamine	2	−5.3	−5.3	−3
desipramine	100	−3.5	−3.5	0.7
famotidine	45	−4.6	−4.3	−0.8
furosemide	61	−4.8	−4.5	−0.7
guanabenz	75	−5.0	−4.4	0.9
HBED	5	−5.1	−5.1	−0.2
hydrochlorothiazide	67	−4.7	−4.2	−0.2
imipramine	99	−3.5	−3.5	1.8
labetalol	90	−4.2	−3.8	0.5
methotrexate	20	−4.7	−4.7	−3
metolazone	64	−4.6	−4.6	4.1
metoprolol	95	−4.2	−4.2	−0.8
phenytoin	90	−4.0	−4.0	2.2
piroxicam	100	−4.0	−3.3	0.3
progesterone	91	−3.8	−3.8	4.3
propranolol	90	−4.4	−4.0	0.8
ranitidine	50	−4.6	−4.5	−1.1
sulfasalazine	13	−4.9	−4.9	−0.7
sulpiride	35	−4.6	−4.6	−1.6
terbutaline	70	−4.1	−4.1	−2
testosterone	100	−3.5	−3.5	3.9
timolol	72	−4.4	−4.2	−0.7
valsartan	55	−5.0	−4.5	−1.6
warfarin	98	−3.8	−3.8	0.6

with $c_D(t)$ being the compound concentration in the donor compartment and $c_R(t)$ being the concentration in the acceptor compartment. In absence of membrane retention P_a is identical to P_e, the effective membrane permeability. When membrane retention occurs P_a can be converted to P_e using mass balance equations.

In a typical experiment, the permeability of propranolol (see structure in Figure 1) at pH 6.8 was assessed. Measuring its absorbance in the solution from the acceptor compartment at 290 nm after 5 h incubation time yielded a value of 0.075 ± 0.001. The reference absorbance at pH 6.8, corresponding to a full equilibrium of the compound after dilution between donor and acceptor compartment, was determined as 0.386. Hence, the ratio r is 0.194 ± 0.003. Inserting r into eq 1 together with the parameters given above results in log P_e = −4.4.

Unstirred Water Layer Correction. The unstirred water layer is an aqueous film at the membrane interface where the solute concentration is purely diffusion-controlled. The unstirred water layer becomes the rate-determining step for the diffusion of highly permeable compounds through membranes.[25,26] As a consequence two molecules with different intrinsic membrane permeability (P_o) may have the same effective permeability (P_e). To correct P_e for the unstirred water layer contribution (P_{ul}), we used the method proposed by Gutknecht and Tosteson.[27−30] Briefly, P_e is related to P_o and P_{ul} as follows:

for a weak base:
$$\frac{1}{P_e} = \frac{[B_t]}{[B]P_o} + \frac{1}{P_{ul}} \qquad (3a)$$

for a weak acid:
$$\frac{1}{P_e} = \frac{[A_t]}{[HA]P_o} + \frac{1}{P_{ul}} \qquad (3b)$$

Results

Thirty-two generic drugs with known human GI-tract absorption were tested for their ability to cross a

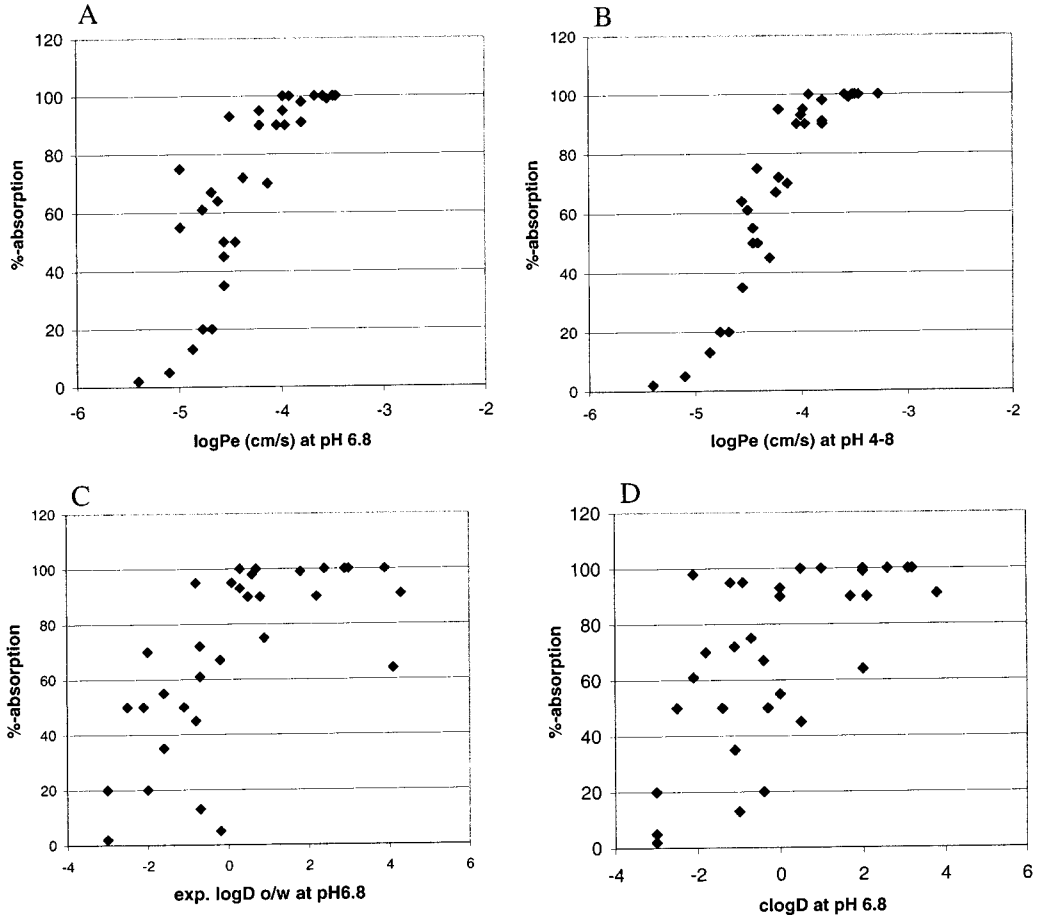

Figure 3. (A) GI-tract absorption of a set of 32 drugs vs HDM log P_e at pH 6.8. (B) Similar to (A) with best permeability within the pH range 4−8 taken into account. (C) Correlation between percent absorption and experimental octanol/water distribution coefficient at pH 6.8. (D) Similar to (C) with calculated distribution coefficients.

hexadecane membrane (HDM). A good correlation was observed between percent absorption and HDM log P_e measured at pH 6.8 (Table 1, Figure 3A). For a number of compounds, however, the HDM log P_e value measured at pH 6.8 leads to an underestimation of the fraction absorbed (guanabenz, furosemide, hydrochlorothiazide, metolazone, and valsartan).

To mimic an environment which more closely resembles the conditions encountered as the substance moves through the GI-tract, permeability measurements were repeated at different pH values, varying from pH 4 to pH 8, and the highest HDM log P_e value was taken into account for each compound (Figure 3B). Comparison of panels A and B in Figure 3 shows that the introduction of the notion of the pH permeability profile significantly improved the correlation between percent absorbed and log P_e.

For comparison, the predictive value of octanol/water distribution coefficients at pH 6.8 was significantly lower than HDM log P_e at the same pH (Figure 3c).

pH Permeability Profiles. Permeability of ionizable compounds strongly depends on the extracellular pH.[31] HDM pH permeability profiles were measured for 16 compounds: 7 weak acids and 9 weak bases. Permeability pH profiles for diclofenac and desipramine are shown in Figure 4. As expected, the permeability of diclofenac increases with increasing acidity (Figure 4a). Interestingly, compared to the ionization curve the effective permeability vs pH curve of diclofenac is shifted to the right with an apparent pK_a of 5.6. As a consequence, significant permeability is measured at pH 7.5 while from the ionization curve the fraction of neutral diclofenac becomes significant only at pH < 6.

Correspondingly, for desipramine the opposite behavior is found (Figure 4b): Compared to the ionization curve, the permeability pH profile is shifted to the left with an apparent pK_a of 6.5. Here again, the compound starts to permeate at pH 5.5 while the neutral species becomes significant only at pH > 8.5. These shifts in the permeability pH profiles are due to the unstirred water layer effect.

Unstirred Water Layer Effect. The rate of absorption of highly permeable compounds is limited by their diffusion through the unstirred water layer associated to the membrane. From eqs 3a and 3b one can estimate the separate contributions of the unstirred water layer (P_{ul}) and the hexadecane layer (P_o) to the overall permeability (P_e). For diclofenac (Figure 4c) one obtains a log P_o of −1.3 and a log P_{ul} of −3.7. Thus, for diclofenac the unstirred water layer becomes the rate-limiting step for permeation of the neutral species. The thickness λ of the combined unstirred water layer can be estimated from the compound's diffusion coefficient D and the unstirred water layer permeability as $\lambda = D/P_{ul}$. With a diffusion coefficient[28] of ca. 6×10^{-6} cm/s one obtains $\lambda = 285$ μm. Log P_o and log P_{ul} were determined in a similar way for desipramine (Figure 4d). Log P_o and log P_{ul} were 0.1 and −3.7, respectively, which yields an

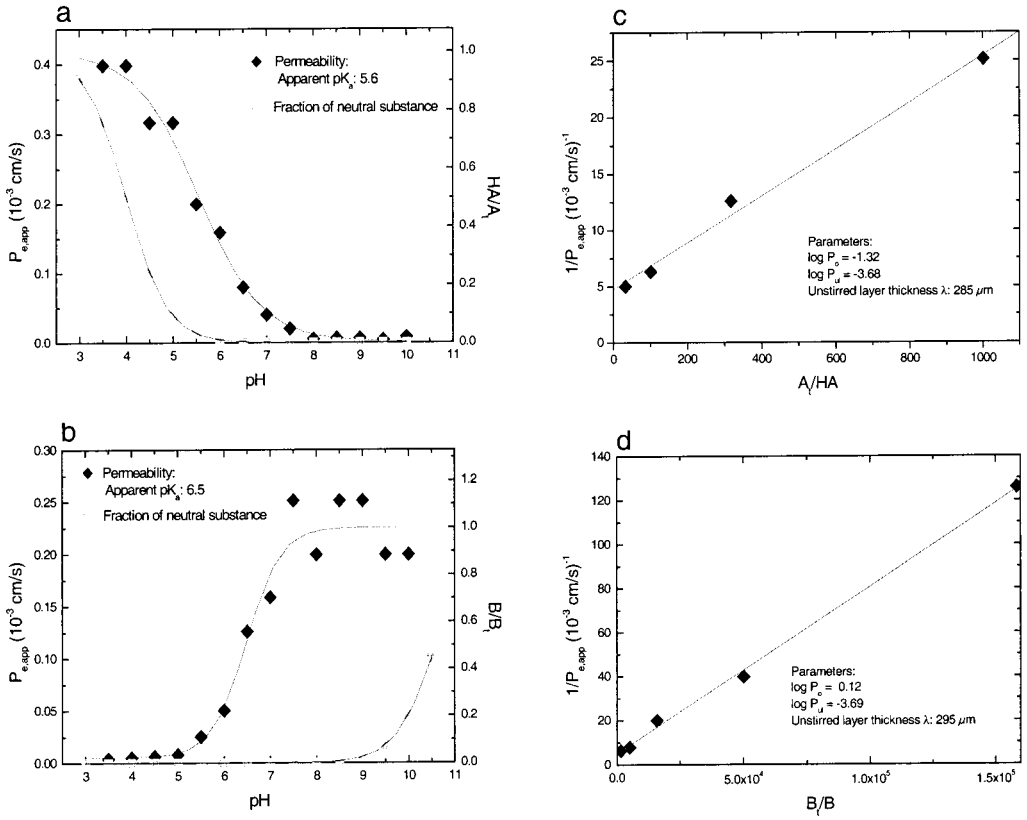

Figure 4. pH-dependent permeability of ionizable compounds: (a) diclofenac (acidic pK_a = 4.0), (b) desipramine (basic pK_a = 10.6), and determination of their permeabilities through the unstirred water layer: (c) diclofenac; (d) desipramine.

Table 2. Maximum Theoretical Effective Permeability for Various Unstirred Water Layer Thickness ($D = 6 \times 10^{-6}$ cm^2/s)

UWL thickness (μm)	LogP$_e$ max (cm/s)	
50	-2.9	← In vivo (GI)
300	-3.7	← HDM
500	-3.9	
800	-4.1	
1500	-4.4	← Caco-2 (unstirred)

unstirred layer thickness of 295 μm. From these experiments one can conclude that our experimental setup is characterized by a combined unstirred water layer of about 300 μm (ca. 150 μm on each side of the membrane), which is consistent with the fact that the highest measured log P_e values were around −3.5 to −3.7 (Table 2).

Discussion

In this paper we describe a novel approach to measure membrane permeability of drug candidates which combines good predictive value and high-throughput. We have shown that permeation across an alkane liquid membrane immobilized between two aqueous phases correlates well with percent absorption in humans (when permeability dictates absorption). The data generated with our training set re-emphasize the importance of permeability pH profile for the prediction of gastrointestinal absorption of ionizable drugs. The assay described in the present manuscript allows the determination of several parameters useful in drug discovery and lead optimization: these are effective membrane permeability (P_e), unstirred water layer controlled permeability ($P_{ul} = P_e$ corrected for ionization), intrinsic membrane permeability ($P_o = P_e$ corrected for ionization and unstirred water layer), and alkane/water partition coefficient.

Permeability pH Profiles. Weakly ionizable compounds have an at least 1000-fold higher membrane permeability in their un-ionized state than when ionized.[27,29] Absorption windows in the GI-tract are defined by the combination of the pH gradient and surface available for absorption. This means that ionizable compounds need to be characterized by their permeability pH profile (Figure 4a,b). Interestingly, the apparent pK_a is shifted by several log units compared to the aqueous pK_a. The explanation for this phenomenon lies in the presence of an unstirred water layer at the hexadecane/water interface. For lipophilic compounds the diffusion through the unstirred water layer becomes the rate-limiting step since it is often several orders of magnitude smaller than the diffusion through the membrane interior. This phenomenon has also been described in Caco-2 monolayer permeation experiments which showed that P_e increased as the thickness of the unstirred water layer was decreased by different stirring techniques.[32]

The knowledge of the permeability pH profile and aqueous pK_a allows the intrinsic membrane permeability P_o to be calculated. To illustrate the impact of the unstirred water layer and ionization on permeability, we calculated P_o and P_{ul} for five highly permeable, ionizable drugs and compared log P_o with HDM log P_e and Caco-2 monolayer effective permeability

Table 3. Effective Permeability Values of Five Highly Permeable, Ionizable Compounds, Measured with Caco-2 Cells, and Their Respective Effective and Intrinsic Permeabilities, Measured with Our HDM Assay

compound	Caco-2 log P_e	HDM log $P_{e,max}$	HDM log P_o
chlorpromazine	−4.7[42]	−3.6	1.3
imipramine	−5.3[43]	−3.7	0.8
desipramine	−4.6[42]	−3.7	0.1
ibuprofen	−4.7[44]	−3.7	−0.9
propranolol	−4.5[44,45]	−3.5	−1.6

(Caco-2 log P_e). Table 3 shows that the maximal effective permeabilities log $P_{e,max}$ are similar for all compounds and equal the maximum theoretical log P_e value predicted for an unstirred layer of 300 μm (Table 2), which means that the unstirred water layer was the rate-limiting step for permeation. Neither HDM log P_e nor Caco-2 log P_e are able to differentiate among these highly permeable compounds since in all cases the experimental permeability is limited by the unstirred water layer. Similarly, log P_e values from Caco-2 cells correspond to the theoretical value calculated for an unstirred water layer of 1500 μm which is the usual unstirred layer thickness reported for unstirred cell culture experiments.[33] In contrast, the intrinsic membrane permeability (P_o) values vary considerably from log $P_o = -1.6$ for propranolol up to log $P_o = 1.3$ for chlorpromazine (Table 3). Evidently, intrinsic permeability allows a ranking of the compounds for membrane permeability while all compounds looked identical for log P_e.

Alkane/Water Partition Coefficients. Interestingly, hexadecane/water partition coefficients can also be derived from the permeability pH profile as membrane permeability is related to membrane partition coefficient:

$$P_o = P_{hxd}(D/h) \quad (4)$$

where P_o is the intrinsic membrane permeability (cm/s), P_{hxd} is the hexadecane/water partition coefficient, D is the diffusion coefficient within the hexadecane membrane (cm^2/s), and h is the membrane thickness (cm). In the log scale eq 4 becomes:

$$\log P_o = \log P_{hxd} + \log(D/h) \quad (5)$$

Figure 5 shows the relation between log P_o and log P_{hxd} obtained experimentally with the 16 compounds of Table 4. The regression line was obtained with a slope of 1.10 and an intercept of 3.03 and gave a correlation coefficient (r^2) better than 0.96. Thus, these data show that measurement of log P_o using the protocol described here allows the determination of log P_{hxd} at least within the range −2 to +5. If one substitutes UV detection (used in this study) by mass spectrometry to quantify the amount of substance in the acceptor compartment, the dynamic range of the method could be further increased, and log $P_{alkane/water}$ values of −3 to −4 could become accessible.

The fact that alkanes can be used to model transcellular passive diffusion is not totally surprising since in the past decade several groups have demonstrated that the bilayer interior is in many respects well-represented by long chain alkanes.[28,34,35] Moreover, a number of studies have reported a good correlation between alkane/water distribution coefficient and permeation across phospholipid bilayers.[35−37] In addition, it has been shown that for compounds within the molecular weight range 200−600 permeability is mainly determined by hydrogen-bonding potential[17] and ionization state, properties which are both modeled by an alkane liquid layer. To check whether the permeability measured with our setup would fit with permeability values obtained with real phospholipid bilayers, we compared the log P_o values we obtained for benzoic acid with values measured earlier by Walter and Gutknecht, using egg PC bilayer membranes (log P_m) formed by the brush technique.[34] For benzoic acid we determined log $P_o = -3.2$ while log P_m was −0.26. To compare log P_o with log P_m one needs to normalize the membrane thickness (see eqs 4 and 5). If one assumes 10 nm for the thickness of a phospholipid bilayer membrane (our HDM membrane is 10 μm thick), then log P_o, normalized to 10 nm, becomes −0.32 and compares favorably with the reported log P_m of −0.26 obtained with egg PC bilayers.

Finally, to assess the value of our approach we compared our data with a number of experimental and theoretical approaches which have been proposed to predict drug absorption.

The octanol/water distribution coefficient (log $D_{o/w}$) is widely used for the prediction of GI-tract absorption of ionizable substances. Comparison of panels A and C in Figure 3 indicates that HDM log P_e is performing better

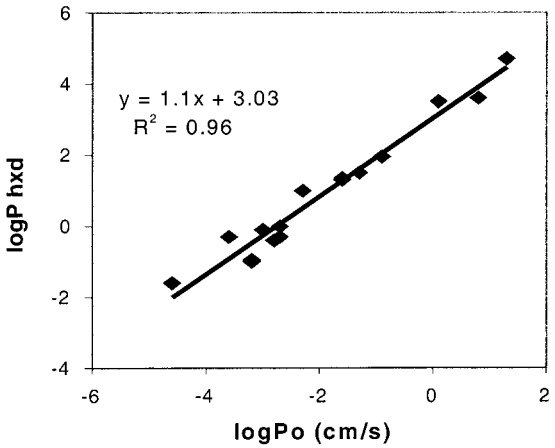

Figure 5. Correlation between membrane intrinsic permeability (log P_o) and alkane/water partition coefficients (log P_{hxd}).

Table 4. Effective Permeability Corrected for Ionization, Intrinsic Permeability, and Hexadecane/Water Partition Coefficients Measured Using the Dual-Phase Titration Method

compound	log $P_{e,max}$	log P_o	log P_{hxd}
alprenolol	−3.6	−1.6	1.3
benzoic acid	−3.3	−3.2	−0.9
chlorpromazine	−3.6	1.3	4.7
desipramine	−3.7	0.1	3.5
diclofenac	−3.7	−1.3	1.5
guanabenz	−4.9	−4.6	−1.6
ibuprofen	−3.7	−0.9	1.95
imipramine	−3.7	0.8	3.6
ketoprofen	−3.6	−2.7	0
metoprolol	−3.6	−2.8	−0.4
naproxen	−3.5	−2.7	−0.3
phenytoin	−4.4	−3.6	−0.3
propranolol	−3.7	−1.6	1.3
salicylic acid	−3.4	−3.2	−1
timolol	−3.6	−3.2	−1.0
warfarin	−3.6	−2.3	1

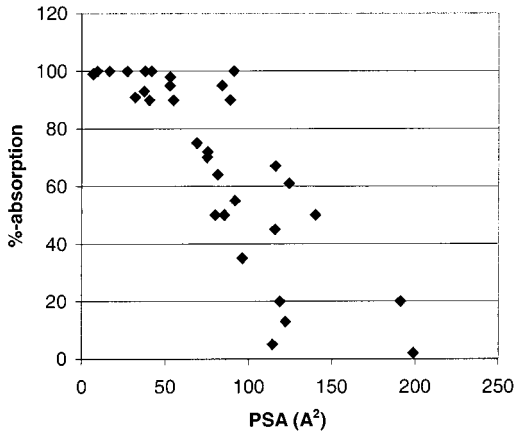

Figure 6. Correlation between PSA and percent absorption.

than log $D_{o/w}$ to predict GI-tract absorption. In particular, sulfasalazine and metolazone are largely overestimated in the octanol/water system. This is most likely due to the inadequate hydrogen bond acidity component of octanol. Indeed, these two substances have a large number of strong hydrogen bond acceptor groups (Figure 1). In addition, experimental determination of log *D* vs pH is rather labor-intensive and therefore not suited for high-throughput.

An alternative to experimental log *D* lies in distribution coefficients obtained from calculated pK_a/log *P* values. As for the experimentally determined distribution coefficients, absorption increases with clog $D_{6.8}$ and reaches a plateau for values > 0 (Figure 3D). The correlation with GI-tract absorption, however, deteriorates compared to the experimental approach.

Figure 6 shows the correlation obtained using PSA as a descriptor to model absorption. When PSA does not exceed 50 Å^2 compounds are all well-absorbed. Within the range 60−120 Å^2 the picture is much more scattered, making solid predictions rather difficult. A number of compounds with different percent absorption showed similar PSA values, like furosemide and sulfasalazine or sulpiride and piroxicam. Likely explanations for the limitations of PSA lie in improper modeling of ionization (and charge distribution) as well as lack of modeling of polarity distribution on the surface of the molecule.

Finally, we want to discuss the value of our artificial membrane model compared to cell culture assays such as the Caco-2 cell monolayer permeability assay which has been established as a method to assess drug absorption in vitro.[7,8] Obviously, the nature of a cell monolayer is closer to the gastrointestinal wall than our liquid alkane membrane. In addition, cells potentially mimic active transport and efflux systems such as P-glycoprotein[38] present in the gut wall. There are, however, a number of issues which limit the potential of this approach and which are better addressed by artificial model membranes: (i) permeability pH profiles are difficult to obtain and restricted to a narrow pH range; (ii) the dynamic range is limited by the unstirred water layer; (iii) cost and labor of cell cultures together with analytics needed to quantify compounds in complex media are hurdles for high-throughput; (iv) inherent variability due to the use of living material makes interlaboratory comparisons difficult.

Conclusion

In this manuscript we presented a novel method to experimentally determine permeability pH profiles which is well-suited for high-throughput screen. Furthermore, it allows the determination of compound properties like effective and intrinsic membrane permeability and possibly hydrogen-bonding potential as well as alkane/water log *P*. In this respect, this is the first experimental high-throughput alkane/water log *P* assay. The liquid alkane membrane does, of course, not model active transport or efflux systems such as P-glycoprotein or multidrug resistance-associated protein (MRP).[39,40] Hence, it is not a replacement for Caco-2 cell monolayers, but rather a complementary method for the preselection of compounds which at a later stage can be tested for their biochemical properties. Finally, when considering GI-tract absorption one should keep in mind that water-soluble substances with molecular weights lower than 200 might cross the GI-tract barrier via the paracellular route while for high-molecular-weight compounds (MW > 600), molecular size becomes rate-limiting. For the latter compounds one may combine the HDM assay with another method which generates a molecular size-related descriptor like the cross-sectional surface area.[41]

Acknowledgment. We thank Mrs. Sabine Arnold for excellent technical assistance.

References

(1) Prentis, R. A.; Lis, Y.; Walker, S. R. Pharmaceutical innovation by the seven UK-owned pharmaceutical companies (1964−1985). *Br. J. Clin. Pharmacol.* **1988**, *25*, 387−396.

(2) Amidon, G. L.; Lennernäs, H.; Shah, V. P.; Crison, J. R. A theoretical basis for a biopharmaceutic drug classification: the correlation of in vitro drug product dissolution and in vivo bioavailability. *Pharm. Res.* **1995**, *12*, 413−420.

(3) Abbreviations: DMSO, dimethyl sulfoxide; GI-tract, gastrointestinal tract; HDM, hexadecane model membrane; P_a, apparent permeability; P_e, effective permeability, i.e., P_a corrected for membrane retention; P_{ul}, permeability through the unstirred water layer, i.e., P_e corrected for ionization; P_o, intrinsic membrane permeability, i.e., P_e corrected for ionization and unstirred water layer; P_m, permeability of phospholipid bilayers; PSA, polar surface area; PVDF, polyvinylidene fluoride.

(4) ter Laak, A. M.; Tsai, R. S.; Donné-Op den Kelder, G. M.; Carrupt, P.-A.; Testa, B.; Timmermann, H. Lipophilicity and hydrogen-bonding of H_1-antihistaminic agents in relation to their central sedative side-effects. *Eur. J. Pharm. Sci.* **1994**, *2*, 373−384.

(5) Caron, G.; Steyaert, G.; Pagliara, A.; Reymond, F.; Crivori, P.; Gaillard, P.; Carrupt, P.-A.; Avdeef, A.; Comer, J.; Box, K. J.; Girault, H. H.; Testa, B. Structure-lipophilicity relationships of neutral and protonated β-blockers. Part I. Intra- and intermolecular effects in isotropic solvent systems. *Helv. Chim. Acta* **1999**, *82*, 1211−1222.

(6) Young, R. C.; Mitchell, R. C.; Brown, T. H.; Ganellin, C. R.; Griffiths, R.; Jones, M.; Rana, K. K.; Saunders: D.; Smith, I. R.; Score, N. E.; Wilks, T. J. Development of a new physicochemical model for brain penetration and its application to the design of centrally acting H_2 receptor histamine antagonists. *J. Med. Chem.* **1988**, *31*, 656−671.

(7) Artursson, P.; Karlsson, J. Correlation between oral drug absorption in humans and apparent drug permeability coefficients in human intestinal epithelial (Caco-2) cells. *Biochem. Biophys. Res. Commun.* **1991**, *175*, 880−885.

(8) Pade, V.; Stavchansky, S. Link between drug absorption solubility and permeability measurements in Caco-2 cells. *J. Pharm. Sci.* **1998**, *87*, 1604−1607.

(9) Camenisch, G.; Folkers, G.; van de Waterbeemd, H. Comparison of passive drug transport through Caco-2 cells and artificial membranes. *Int. J. Pharm.* **1997**, *147*, 61−70.

(10) Benz, R.; Fröhlich, O.; Läuger, P.; Montal, M. Electrical capacity of black lipid films and of lipid bilayers from monolayers. *Biochim. Biophys. Acta* **1975**, *394*, 325−334.

(11) Fettiplace, R.; Andrews, D. M.; Haydon, D. A. The thickness, composition and structure of some lipid bilayers and natural membranes. *J. Membr. Biol.* **1971**, *5*, 277−296.

(12) Montal, M.; Mueller, P. Formation of bimolecular membranes from lipid monolayers and a study of their electrical properties. *Proc. Natl. Acad. Sci. U.S.A.* **1972**, *69*, 3561−3566.
(13) White, S. H.; Thompson, T. E. Capacitance, area, and thickness variations in thin lipid films. *Biochim. Biophys. Acta* **1973**, *323*, 7−22.
(14) Mountz, J. M.; Tien, H. T. Photoeffects of pigmented lipid membranes in a microporous filter. *Photochem. Photobiol.* **1978**, *28*, 395−400.
(15) Thompson, M.; Lennox, R. B.; McClelland, R. A. Structure and electrochemical properties of microfiltration filter-lipid membrane systems. *Anal. Chem.* **1982**, *54*, 76−81.
(16) Kansy, M.; Senner, F.; Gubernator, K. Physicochemical high throughput screening: parallel artificial membrane permeation assay in the description of passive absorption processes. *J. Med. Chem.* **1998**, *41*, 1007−1010.
(17) van de Waterbeemd, H.; Camenisch, G.; Folkers, G.; Chretien, J. R.; Raevsky, O. A. Estimation of blood-brain barrier crossing of drugs using molecular size and shape, and H-bonding descriptors. *J. Drug Target.* **1998**, *6*, 151−165.
(18) Clarke, F. H.; Cahoon, N. M. Ionization constants by curve fitting: determination of partition and distribution coefficients of acids and bases and their ions. *J. Pharm. Sci.* **1987**, *76*, 611−620.
(19) Avdeef, A. pH-metric logP. Part 1. Difference plots for determining ion-pair octanol−water partition coefficients of multiprotic substances. *Quant. Struct.-Act. Relat.* **1992**, *11*, 510−517.
(20) van de Waterbeemd, H.; Kansy, M. Hydrogen-bonding capacity and brain penetration. *Chimia* **1992**, *46*, 299−303.
(21) Palm, K.; Luthman, K.; Ungell, A.-L-; Strandlund. G.; Artursson, P. Correlation of drug absorption with molecular surface properties. *J. Pharm. Sci.* **1996**, *85*, 32−39.
(22) Palm, K.; Stenberg, P.; Luthman, K.; Artursson, P. Polar molecular surface properties predict the intestinal absorption of drugs in humans. *Pharm. Res.* **1997**, *14*, 568−571.
(23) Winiwarter, S.; Bonham, N. M.; Ax, F.; Hallberg, A.; Lennernäs, H.; Karlén, A. Correlation of human jejunal permeability (in vivo) of drugs with experimentally and theoretically derived parameters. A multivariate data analysis approach. *J. Med. Chem.* **1998**, *41*, 4939−4949.
(24) Adam, G.; Läuger, P.; Stark, G. *Physikalische Chemie und Biophysik*, 2nd ed.; Springer-Verlag: Berlin, 1988; pp 299ff.
(25) Pohl, P.; Saparov, S. M.; Antonenko, Y. N. The size of the unstirred layer as a function of the solute diffusion coefficient. *Biophys. J.* **1998**, *75*, 1403−1409.
(26) Mierle, G. The effect of cell size and shape on the resistance of unstirred layers to solute diffusion. *Biochim. Biophys. Acta* **1985**, *812*, 835−839.
(27) Gutknecht, J.; Tosteson, D. C. Diffusion of weak acids across lipid bilayer membranes: effects of chemical reactions in the unstirred layers. *Science* **1973**, *182*, 1258−1261.
(28) Walter, A.; Gutknecht, J. Monocarboxylic acid permeation through lipid bilayer membranes. *J. Membr. Biol.* **1984**, *77*, 255−264.
(29) Gutknecht, J.; Walter, A. Histamine, theophylline and tryptamine transport through lipid bilayer membranes. *Biochim. Biophys. Acta* **1981**, *649*, 149−154.
(30) Xiang, T.-X.; Anderson, B. D. The relationship between permeant size and permeability in lipid bilayer membranes. *J. Membr. Biol.* **1994**, *140*, 111−122.
(31) Lowther, N.; Tomlinson, B.; Fox, R.; Faller, B.; Sergejew, T.; Donnelly, H. Caco-2 cell permeability of a new (hydroxybenzyl)-ethylendiamine and iron chelator: correlation with physicochemical properties and oral activity. *J. Pharm. Sci.* **1998**, *87*, 1041−1045.
(32) Hidalgo, I. J.; Hillgren, K. M.; Grass, G. M.; Borchardt, R. T. Characterization of the unstirred water layer in Caco-2 cell monolayers using a novel diffusion apparatus. *Pharm. Res.* **1991**, *8*, 222−227.
(33) Karlsson, J.; Artursson, P. A method for the determination of cellular permeability coefficients and aqueous boundary layer thickness in monolayers of intestinal epithelial (Caco-2) cells grown in permeable filter chambers. *Int. J. Pharm.* **1991**, *71*, 55−64.
(34) Walter, A.; Gutknecht, J. Permeability of small nonelectrolytes through lipid bilayer membranes. *J. Membr. Biol.* **1986**, *90*, 207−217.
(35) Venable, R. M.; Zhang, Y.; Hardy, B. J.; Pastor, R. W. Molecular dynamics simulations of a lipid bilayer and of hexadecane: an investigation of membrane fluidity. *Science* **1993**, *262*, 223−226.
(36) Miron, T.; Rabinkov, A.; Mirelman, D.; Wilchek, M.; Weiner, L. The mode of action of allicin: its ready permeability through phospholipid membranes may contribute to its biological activity. *Biochim. Biophys. Acta* **2000**, *1463*, 20−30.
(37) Stein, W. D. *Transport and Diffusion across Cell Membranes*, 1st ed.; Academic Press: San Diego, 1985.
(38) Karlsson, J.; Kuo, S. M.; Ziemniak, J.; Artursson, P. Transport of celiprolol across human intestinal epithelial (Caco-2) cells: mediation of secretion by multiple transporters including P-glycoprotein. *Br. J. Pharmacol.* **1993**, *110*, 1009−1016.
(39) Seelig, A. A general pattern for substrate recognition by P-glycoprotein. *Eur. J. Biochem.* **1998**, *251*, 252−261.
(40) Seelig, A.; Li, X. L.; Wohnsland, F. Substrate recognition by P-glycoprotein and the multidrug resistance-associated protein MRP1: a comparison. *Int. J. Clin. Pharmacol. Ther.* **2000**, *38*, 111−121.
(41) Seelig, A.; Gottschlich, R.; Devant, R. M. A method to determine the ability of drugs to diffuse through the blood-brain barrier. *Proc. Natl. Acad. Sci. U.S.A.* **1994**, *91*, 68−72.
(42) Yazdanian, M.; Glynn, S. L.; Wright, J. L.; Hawi, A. Correlating partitioning and Caco-2 cell permeability of structurally diverse small molecular weight compounds. *Pharm. Res.* **1998**, *15*, 1490−1494.
(43) Unpublished data.
(44) Chong, S.; Dando, S. A.; Morrison, R. A. Evaluation of Biocoat intestinal epithelium differentiation environment (3-day cultured Caco-2 cells) as an absorption screening model with improved productivity. *Pharm. Res.* **1997**, *14*, 1835−1837.
(45) Grès, M.-C.; Julian, B.; Bourrie, M.; Meunier, V.; Roques, C.; Berger, M.; Boulenc, X.; Berger, Y.; Fabre, G. Correlation between oral drug absorption in humans, and apparent drug permeability in TC-7 cells, a human epithelial intestinal cell line: comparison with the parental Caco-2 cell line. *Pharm. Res.* **1998**, *15*, 726−733.

JM001020E